N79-17480

# A Dual-Loop Model of the Human Controller

Ronald A. Hess

NASA Ames Research Center, Moffett Field, Calif.

## Theme

It is the thesis of this paper[1] that a representative model of the human controller in single-axis compensatory tracking tasks should exhibit an internal feedback loop which is not evident in single-loop models now in common use[2]. This hypothetical inner-loop involves a neuromuscular command signal derived from the time rate of change of controlled element output which is due to control activity. It is not contended that the single-loop human controller models now in use are incorrect, but that they contain an implicit but important internal loop closure, which, if explicitly considered, can account for a good deal of the adaptive nature of the human controller in a systematic manner.

## Contents

Figure 1 is a block diagram representation of the hypothetical human controller model. This is referred to as the dual-loop model to distinguish it from typical single-loop structures. The dual-loop model is not derived from any physiological imperatives but rather stems from a structurally similar but philosophically different model discussed briefly by Smith[3]. Table 1 presents the parameters associated with the model of Fig. 1. The equalization $Y_{p_e}$ contains a simple first-order lead term and a high frequency lag term with break frequency $1/T_e$ beyond the undamped natural frequency $\omega_n$ of the neuromuscular system. The exponent 'a' on the lag is included to implement more rapid fall-off in the filtering characteristics of $Y_{p_e}$, if necessary.

The equalization $Y_{p_m}$ consists of a low frequency washout which, in terms of an acceptable feedback control system, is essential for inner-loop low frequency remnant suppression. Inner-loop low frequency remnant power can arise from a variety of sources including errors in the controller's internal model of manipulator/controlled element dynamics $\hat{Y}_\delta Y_c$ at low frequencies, poor kinesthetic feedback $u_\delta$ at low frequencies or broadband process noise. Just as in $Y_{p_e}$, the integer exponent 'b' can be used to implement sharper washout characteristics, if necessary. As Table 1 indicates, the $\hat{Y}_\delta Y_c$ element represents the human controller's internal model of the manipulator/controlled element dynamics. Indeed, the dominant adaptive feature of the dual-loop model is the explicit appearance of $\hat{Y}_\delta Y_c$ in the equivalent single-loop form of the model in Table 1 ($Y_p$).

The element $Y_{p_n}$ represents the neuromuscular dynamics of the particular limb which drives the manipulator. The dynamics shown in Table 1 have been deliberately simplified from the more elaborate neuromuscular model presented in ref. 2 for the sake of simplicity. The remnant signals $r_e$ and $r_{\dot{u}_\delta}$ are injected into displayed error $e_d$ and rate of change of control force $\dot{u}_\delta$. These remnant signals are part of the quasi-linear representation of the outer and inner-loop human controller characteristics.

Implicit in the dual-loop formulation is the assumption that the structure as outlined in Table 1 is complete, i.e., no additions have to be made or restructuring undertaken to account for human controller adaptation to various controlled elements, displays, manipulators, etc. The adaptive potential of the model is contained in the parameters of the inner and outer-loop equalization and in the internal manipulator/controlled element model $\hat{Y}_\delta Y_c$. Four hypotheses

regarding the general adaptive characteristics of the parameterized dual-loop model are offered: Hypothesis 1 - The parameters $K_e$, $K_m'$, and $T_m'$ act in consort with the internal model of the manipulator/controlled element dynamics $\hat{Y}_\delta Y_c$ to define the essential adaptive capabilites of the dual-loop model. The lead equalization in $Y_{p_e}$ is used only when the previous parameters are unable to provide the effective lead equalization which may be required in a specific task. Hypothesis 2 - The relative utilization of the inner and outer-loops of the dual-loop model is a function of manipulator/controlled element dynamics and the quality of the sensory inputs $e_d$ and $u_\delta$. Hypothesis 3 - Relative loop utilization in the dual-loop model can be quantified by the ratio $K_m'/K_e$. Hypothesis 4 - The value of $T_m'$ is determined by the extent to which the inner-loop is utilized and by the quality of the internal model of the manipulator/controlled element dynamics $\hat{Y}_\delta Y_c$. The more the inner-loop is utilized, the larger the value of $T_m'$. The more precise the internal model, the larger the value of $T_m'$. No hypotheses regarding the adaptive nature of the parameters $T_e$ (or $\tau$), $\zeta_n$ and $\omega_n$ are offered. These parameters effect primarily the high frequency portion of the controller describing function $Y_p$ ($\omega > 10$ rad/sec). Since measured data tends to be scant in this frequency range, verifying hypotheses regarding parameter variations would be difficult.

The dual-loop model just outlined can produce describing functions which closely approximate those measured in laboratory tracking tasks. The tasks used in the initial validation involved the following controlled element dynamics: K, K/s, $K/(s)^2$, $K/(s^3+12.3s^2+11.6s)$ and $K/s(s-1)$. In addition, an empirical remnant model utilizing a pair of dual-loop model parameters can approximate the measured error remnant spectra for those experiments for which error injected remnant data were reported (all but the fourth task above).

No formal numerical algorithm was utilized in identifying the dual-loop model parameters for the five experimental tasks. Instead, small and large bandwidth approximations to the last equation in Table 1 were derived and a straight-forward hand-fit procedure was employed for parameter selection and adjustment. The pertinent expressions for $Y_p$ are, for small bandwidth

$$Y_p = u_\delta/e_d \doteq \frac{K_e(T_m's+1)(T_Ls+1)}{(K_m'\hat{Y}_\delta Y_c)s^2+(T_m')s+1} \tag{1}$$

and for large bandwidth

$$Y_p = u_\delta/e_d \doteq \frac{K_e(T_m's+1)(T_Ls+1)e^{-\tau s}}{(T_m'/\omega_n^2)s^3+(2\zeta_nT_m'/\omega_n+K_m'\hat{Y}_\delta Y_c+1/\omega_n^2)s^2+(T_m'+2\zeta_n/\omega_n)s+1} \tag{2}$$

Relations (1) and (2) and the general guidelines of the four hypotheses just stated, allow rapid "identification" of the dual-loop model parameters using measured describing function data through the following two-step process. First, $K_e$, $K_m'$, $T_m'$ and, if necessary, $T_L$ are selected using equation (1) and the low to mid-frequency ($\omega < \omega_c$ where $\omega_c$ is the open-loop crossover frequency) describing function data. Second, $\zeta_n$, $\omega_n$ and $\tau$ are chosen using equation (2), the selected values of $K_e$, $K_m'$, $T_m'$ and $T_L$, and the high frequency ($\omega > \omega_c$) describing function data.

An empirical expression for the normalized power spectral density of the "equivalent" remnant which is injected into the displayed error of the dual-loop model can be obtained from the measured remnant data as

$$\Phi_{nn_e}/\sigma_e^2 = \frac{P_e(K_m'/K_e)}{1+(K_m'/K_e)^2\omega^2/2} \tag{3}$$

where $\sigma_e$ is the root-mean-square value of the displayed error signal and

$P_e$ is a parameter to account for the fact that different levels of human controller attention are required for different control tasks. Only two values of $P_e$ are needed to match the measured remnant data in this study: $P_e = 0.2$ to represent a "low" attention level and $P_e = 0.04$ to represent a "high" attention level.

The dual-loop model can explain the effects of specific display and manipulator variations on human controller characteristics. For example, Fig. 2 shows a comparison between measured and model generated describing functions and remnant spectra for a tracking task with K/s controlled element dynamics and a peripheral display. The match is quite acceptable. In particular, the remnant model does an excellent job of matching the experimental remnant spectrum in spite of the fact that the former was empirically derived from foveal viewing data.

The assessment of a dual-loop model of the human controller undertaken in this study leads to the following conclusions: (1) The proposed dual-loop model and the general adaptive characteristics which have been hypothesized can produce human controller describing functions which closely approximate those measured in a wide variety of single-axis compensatory tracking tasks. (2) An empirical model for injected remnant spectra employing low and high controller attention levels can approximate experimentally derived injected remnant spectra. Of the experiments to which the remnant models were applied, the low attention model satisfactorily matched the data for the stable controlled elements while the high attention model matched the data for the unstable elements. (3) The dual-loop model and associated hypotheses can explain the measured variations in human controller dynamics and performance which accompany changes in controlled element dynamics and variations in display and manipulator characteristics. (4) In terms of existing single-loop models, the dual-loop model exhibits the following novel features: (a) the adaptive nature of the model is due primarily to the existence of an explicit internal model of the manipulator/controlled element dynamics in an inner feedback loop, (b) in controlling all but the most difficult controlled element, the dual-loop model indicates that the necessity of lead equalization in the form of error rate utilization is obviated, i.e., in all but one case, $T_L = 0$. Likewise, apparent error lag equalization for pure gain controlled elements is accomplished by inner-loop activity.

## References


[1]Hess, R. A., "A Dual-Loop Model of the Human Controller in Single-Axis Compensatory Tracking Tasks," NASA TM-73,249, May 1977

[2]McRuer, D. T., "Development of Pilot-in-the-loop Analysis," Journal of Aircraft, Vol. 10, Sept. 1973, pp. 515-524.

[3]Smith, R. H., "A Unified Theory for Pilot Opinion Rating," Proceedings of the Twelfth Annual Conference on Manual Control, NASA TM X-73,170, May 1976, pp. 542-558.

Table 1. Dual-Loop Model Parameters

| Model Element | Form | Description |
|---|---|---|
| $Y_{p_e}$ | $\frac{K_e(T_L s+1)}{(T_e s+1)^a}$ | displayed error equalization<br>a = 1,2, . . |
| $Y_{p_{\dot{m}}}$ | $\frac{K_{\dot{m}} s^b}{(T_{\dot{m}} s+1)^b}$ | control rate equalization<br>b = 1,2, . . |
| $\hat{Y}_\delta Y_c$ | | human controller's internal model of manipulator/controlled element dynamics |
| $Y_{p_n}$ | $\frac{1}{(s/\omega_n)^2+(2\zeta_n/\omega_n)s+1}$ | neuromuscular dynamics |
| $r_e$, $r_{\dot{u}_\delta}$ | | remnant injected into displayed error and control rate, respectively |
| $Y_p = u_\delta/e_d$ | $\frac{Y_{p_e} Y_{p_n}}{1+Y_{p_n}\hat{Y}_\delta Y_c Y_{p_{\dot{m}}} s}$ | equivalent single-loop human controller describing function |



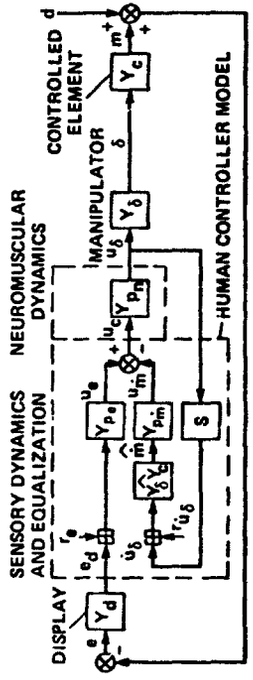


Figure 1. Quasi-Linear Dual-loop Model of the Human Controller in a Single-Axis Compensatory Tracking Task

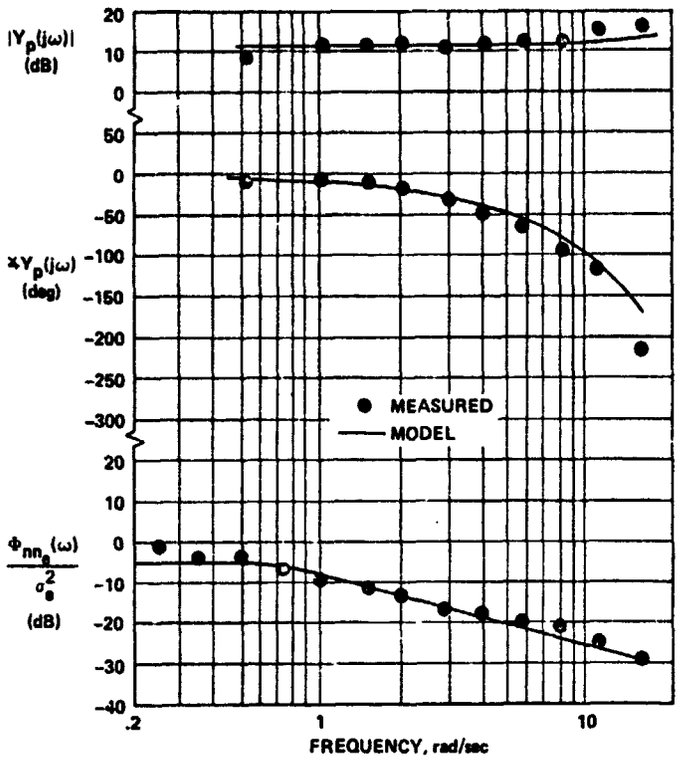


Figure 2. Comparison Between Measured and Dual-Loop Describing Functions and Injected Remnant Spectra for K/s Dynamics and 22° Peripheral Viewing